Magnetic structures in the ternary RM_2X_2 compounds (R = Gd to Tm; M = Fe, Co, Ni, or Cu; X = Si or Ge)

H. Pinto, M. Melamud, and M. Kuznietz
Nuclear Research Centre—Negev, P.O. Box 9001, Beer-Sheva 84190, Israel

H. Shaked
Nuclear Research Centre—Negev, P.O. Box 9001, Beer-Sheva 84190, Israel
and Ben-Gurion University of the Negev, P.O. Box 653, Beer-Sheva 84105, Israel
(Received 3 July 1984)

Neutron-diffraction measurements were performed on polycrystalline samples of 13 different compounds of the type RM_2X_2 (R, a heavy lanthanide from Gd to Tm; M, the $3d$ element Fe, Co, Ni, or Cu; X, Si or Ge), at room temperature and at low temperatures. The crystallographic structure of these compounds belongs to the tetragonal space group $I4/mmm$ (D_{4h}^{17}). It was found that these compounds, paramagnetic at room temperature, undergo a transition to antiferromagnetism at low temperatures. The transition temperatures and most of magnetic structures were determined. Below the transition temperature, magnetic ordering was found only on the R sublattice, and no magnetic ordering was detected on the M sublattice. The magnetic lattices were found to be characterized by propagation vectors of $\vec{k}=(0,0,1)$ in the cobalt compounds investigated ($TbCo_2Si_2$, $HoCo_2Si_2$, $DyCo_2Ge_2$, and $ErCo_2Ge_2$), $\vec{k}=(\frac{1}{2},0,\frac{1}{2})$ in the copper compounds investigated ($TbCu_2Si_2$, $HoCu_2Si_2$, $TbCu_2Ge_2$, and $HoCu_2Ge_2$), and incommensurate $\vec{k}=(0,0,0.76)$ in $HoNi_2Ge_2$ (unsolved incommensurate in other nickel compounds and in iron compounds). Together with previously published results on other RM_2X_2 compounds, the magnetic lattice is found to vary with M and be almost invariant to R.

I. INTRODUCTION

Polycrystalline samples of the ternary compounds of the composition AB_2X_2 (A, a lanthanide or actinide; B, a $3d$, $4d$, or $5d$ transition element; X, silicon or germanium) have been extensively studied by x-ray diffraction.[1–15] All these compounds were found to be isostructural with the ordered $BaAl_4$-type tetragonal structure [space group $I4/mmm$ (D_{4h}^{17}); Ref. 16]. The tetragonal unit cell is approximately $4\times4\times10$ Å^3 for all compounds ($c/a\sim2.5$), and contains two formula units (Fig. 1). The atoms A, B, and X occupy the positions $2a$, $4d$, and $4e$, having the point-group symmetries $4/mmm$, $\bar{4}m2$, and $4mm$, respectively.[16] In the LnB_2X_2 compounds (Ln denotes lanthanide), the crystallographic properties vary slowly and monotonically across the lanthanide series,[3,5–8,10,12,14,15] with only Ce, Eu, and Yb forming some exceptions to this rule.

Magnetic susceptibilities have been measured as a function of temperature in many of the AB_2X_2 compounds.[13,15,17–32] Many of the investigated compounds were found, upon cooling, to undergo magnetic transitions into ordered states: ferromagnetic, antiferromagnetic, and ferrimagnetic. Some of these compounds undergo several transitions.[13,29,32] Neutron-diffraction studies of AB_2X_2 compounds have been reported.[33–57] In most magnetically ordered compounds, the A sublattice was found to be ordered, but in some cases ordering was found also on the B sublattice or on both sublattices.[22,34,41,53] In the neutron-diffraction studies of the compounds with A-sublattice or-

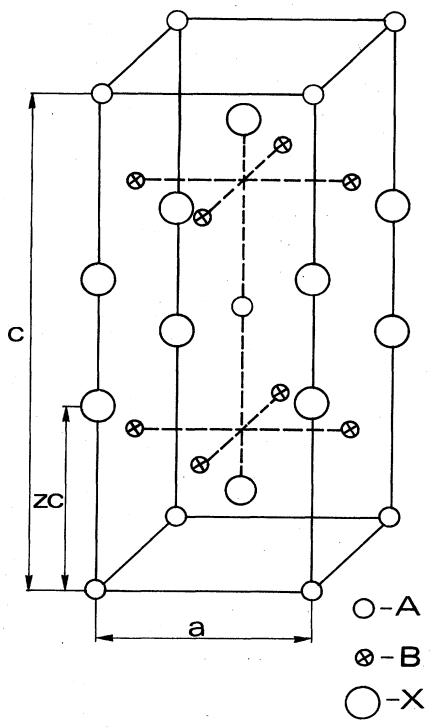

FIG. 1. Crystallographic unit cell of the ternary AB_2X_2 compounds with the atoms A, B, and X occupying the $2a$, $4d$, and $4e$ positions ($z\sim\frac{3}{8}$), respectively, belonging to the space group $I4/mmm$ (ordered $BaAl_4$-type tetragonal structure).

dering, ferromagnetic and antiferromagnetic structures were found, the latter being commensurate or incommensurate with the tetragonal crystallographic lattice. In the commensurate antiferromagnetic compounds, propagation vectors, $\vec{k}=(0,0,1)$, $(0,0,\frac{1}{2})$, $(\frac{1}{2},0,\frac{1}{2})$, $(\frac{1}{2},\frac{1}{2},0)$, and $(\frac{1}{2},\frac{1}{2},\frac{1}{2})$, were observed, with the corresponding doubling of the tetragonal translation, in zero, one, two, two, and three directions, respectively (the latter being reported in Ref. 54).

Some of the magnetic results were corroborated by Mössbauer-effect studies.[9,13,23,32,36,58–66] Thus fast magnetic fluctuations (in $EuCu_2Si_2$) were observed.[58] Second-order magnetic transitions were observed in some compounds,[33,36] and first-order ones in others.[23] One therefore deals with a variety of magnetic properties in the AB_2X_2 compounds. Recently, single crystals of $TbRh_2Si_2$ and $CeCu_2Si_2$ were prepared and studied by magnetic measurements.[55,67]

In the present work we confine ourselves to the RM_2X_2 compounds (R, a heavy lanthanide from Gd to Tm; M, a $3d$ element Fe, Co, Ni, or Cu; X, Si or Ge), a total of 48 compounds. Many of these compounds have been studied and found to be antiferromagnetic. We report our neutron-diffraction results for the following 13 compounds: $TbFe_2Si_2$, $TbCo_2Si_2$, $HoCo_2Si_2$, $HoNi_2Si_2$, $TbCu_2Si_2$, $HoCu_2Si_2$, $TbFe_2Ge_2$, $DyCo_2Ge_2$, $ErCo_2Ge_2$, $TbNi_2Ge_2$, $HoNi_2Ge_2$, $TbCu_2Ge_2$, and $HoCu_2Ge_2$. In several of these compounds preliminary results are reported. While the present research was in progress, neutron-diffraction results obtained in other laboratories were published for $TbCo_2Si_2$ (Refs. 40, 45, and 46), $HoCo_2Si_2$ (Refs. 45, 46, and 48), and $ErCo_2Ge_2$ (Ref. 47).

In Sec. II we report experimental details on sample preparation and characterization, and the determination of magnetic structures. In Sec. III we report our experimental results. In Sec. IV we discuss our results in the context of the systematics within the RM_2X_2 system of compounds.

II. EXPERIMENTAL DETAILS

A. Sample preparation and characterization

Powder samples of the RM_2X_2 compounds were synthesized by arc-melting, under argon atmosphere, of stoichiometric amounts of the R, M, and X elements with purities of 99.9% or higher. All the samples were characterized by x-ray diffraction, using Cu $K\alpha$ radiation. Several of the samples were annealed in vacuum for 5 d at 800 °C. No change was obtained in either room-temperature or low-temperature diffraction patterns, except for the $TbCu_2Ge_2$ sample, where annealing affected the low-temperature pattern. For all samples prepared, the x-ray-diffraction patterns (mainly at room temperature) yielded the correct crystallographic structure, with lattice parameters in agreement with the published values.[3,7,8,12,20,21,24,29,40,45–48] Additional weak x-ray reflections in some compounds indicated the presence of impurities or small amounts of foreign phases. These reflections were also found in the neutron-diffraction patterns, where they appeared to be weak, did not show any change with temperature, and did not interfere with the low-temperature magnetic reflections. We therefore disregarded these additional reflections.

All powder samples used in the neutron-diffraction measurements were encapsulated in cylindrical aluminum cans (14 mm in diameter), except for the $DyCo_2Ge_2$ sample, which was encapsulated in a flat sample holder (2 mm thick), the absorption correction factor D for this sample being ~ 2.4 (Ref. 43) (which corresponds to an effective thickness of 1.5 mm).

The neutron-diffraction measurements were performed at the IRR-2 reactor (at NRC-Negev) using neutrons with a wavelength $\lambda \sim 2.45$ Å. The $\lambda/2$ component was removed from the beam using a 52 mm thick highly oriented pyrolytic graphite filter. The room-temperature neutron-diffraction patterns were analyzed using a least-squares program which "best fitted" the calculated to the observed integrated intensities. These analyses yielded structural parameters in agreement with those published earlier.

B. Determination of magnetic structures

In order to investigate the magnetic structures of the various compounds prepared, neutron-diffraction patterns

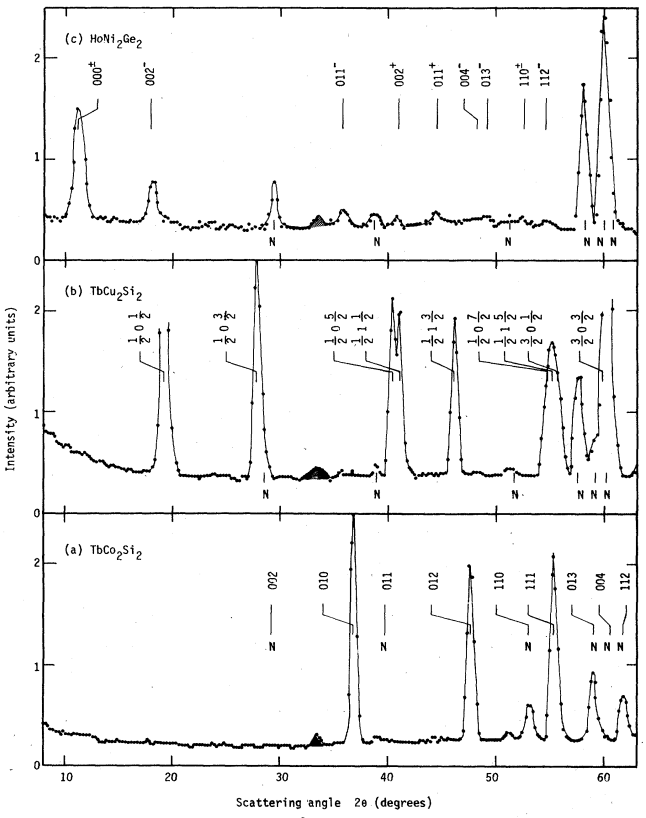

FIG. 2. Neutron- (~ 2.45 Å) diffraction patterns at low temperatures, for three representative magnetic structures in the RM_2X_2 compounds investigated in the present study. (a) $TbCo_2Si_2$ at 4.2 K, with $\vec{k}=(0,0,1)$ [see configuration in Fig. 4(a)]—crystallographic lines indexed; (b) $TbCu_2Si_2$ at 4.2 K, with $\vec{k}=(\frac{1}{2},0,\frac{1}{2})$ [see configuration in Fig. 4(b)]—crystallographic lines as in (a); (c) $HoNi_2Ge_2$ at 2.1 K, with $\vec{k}=(0,0,0.76)$ (incommensurate magnetic configuration)—crystallographic lines as in (a). N denotes allowed crystallographic lines.

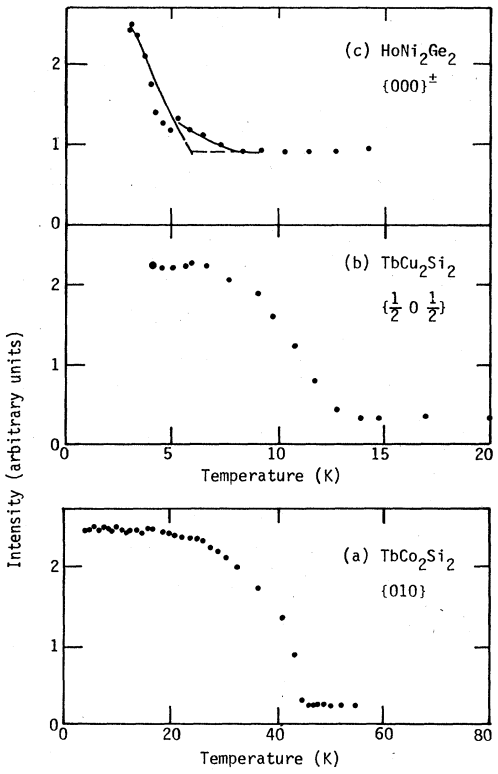

FIG. 3. Peak intensity versus temperature curves for the three representative RM_2X_2 compounds of Fig. 2. (a) $TbCo_2Si_2$—{010} magnetic reflection; (b) $TbCu_2Si_2$—$\{\frac{1}{2}\ 0\ \frac{1}{2}\}$ magnetic reflection; (c) $HoNi_2Ge_2$—$\{000\}^{\pm}$ magnetic reflection.

($\lambda \sim 2.45$ Å) were obtained at 4.2 K (liquid-helium temperature), or at 2.1 or 1.9 K (pumped-liquid-helium temperature), in cases of low magnetic ordering temperatures, ensuring as large magnetic moments as possible.

In Fig. 2 three low-temperature patterns are shown for $TbCo_2Si_2$, $TbCu_2Si_2$, and $HoNi_2Ge_2$, as examples of the diversity of magnetic structures found in the investigated compounds. Compared with the corresponding room-temperature patterns, the low-temperature patterns of all three compounds included extra reflections. These are the magnetic reflections which result from the ordered magnetic lattice. The corresponding propagation vectors $\vec{k}$ were found and the patterns indexed accordingly. The $\vec{k}$ vectors found for the various compounds were commensurate or incommensurate with the crystallographic unit cell. The magnetic structures (moment direction and magnitude, and possible modulation) were calculated by least-squares fitting of the calculated to the observed integrated intensities. We used for the magnetic form factor the approximation $f=\exp(-C\sin^2\theta/\lambda^2)$, consistent with Freeman and Watson,[68] with C values of 4.8, 3.83, and 3.83 Å^2 for terbium, dysprosium, and holmium, respectively. The transition temperatures were obtained from plots of peak intensity versus temperature of at least one magnetic reflection for each compound. Examples of such measurements (for the compounds of Fig. 2) are given in Fig. 3.

III. RESULTS

The experimental results of the neutron-diffraction study of the 13 RM_2X_2 compounds are given in Tables I and II. The structural analysis, including the lattice parameters and the weighted R factors, both at room and liquid-helium temperatures, was carried out to date in full only for several of the RM_2X_2 compounds, and the results are listed in Table I. The measured Néel temperatures (T_N) for all 13 compounds are given in Table II. In $HoNi_2Si_2$ and $TbNi_2Ge_2$, there are indications for a second magnetic transition below T_N. The magnetic structure parameters, except for four iron and nickel compounds, for whom the magnetic structures are incommensurate with the crystallographic unit cell and have yet to be solved, are given also in Table II. These parameters include the $\vec{k}$-propagation vector and the direction and magnitude of the magnetic moment. Magnetic ordering was found only on the R sublattice, and no magnetic ordering was detected on the M sublattice. In the nine compounds where the $\vec{k}$ vector was determined it is (0,0,1) in four cases (all cobalt compounds), $(\frac{1}{2},0,\frac{1}{2})$ in four other cases (all copper compounds), and (0,0,0.76) (i.e., incommensurate) in one case, namely $HoNi_2Ge_2$. The magnitude of magnetic moment was determined in six com-

TABLE I. Crystallographic parameters and weighted R factors obtained for several RM_2X_2 compounds from neutron-diffraction patterns at room and liquid-helium temperatures.

	Parameters at 300 K				Parameters at 4.2 K			
Compound	a (Å)	c (Å)	z	R^a (%)	a (Å)	c (Å)	z	R^a (%)
$TbCo_2Si_2$	3.896	9.766	0.371	7.7	3.888	9.746	0.369	5.6
$TbCu_2Si_2$	3.988	9.966	0.383	2.8	3.984	9.947	0.385	3.9
$HoCu_2Si_2$	3.966	9.977	0.382	6.0	3.950	9.977	0.374	7.0
$DyCo_2Ge_2$[b]	3.966	10.024	0.372	10.2	3.966	10.024	0.373	14.7
$TbCu_2Ge_2$[c]	4.044	10.266	0.381	3.5	4.044	10.266	0.380	3.8

[a] $R=100(\{\sum[(I_{obs}-I_{calc})/\sigma]^2\}/[\sum(I_{obs}/\sigma)^2])^{1/2}$, where σ is the experimental error in I_{obs}.
[b] Lattice parameters from Ref. 7.
[c] Lattice parameters from Ref. 3.

TABLE II. Transition temperatures T_N and the magnetic structure parameters for the 13 RM_2X_2 compounds investigated in the present study.

Compound	T_N (K)	Magnetic structure parameters $\vec{k}$	$\vec{\mu}$ direction	μ(4.2 K) (μ_B)
$TbFe_2Si_2$	10.5	Incommensurate		
$TbCo_2Si_2$[a]	46	(0,0,1)	$\parallel\vec{c}$	9.2
$HoCo_2Si_2$[b]	10.2	(0,0,1)	$\parallel\vec{c}$	
$HoNi_2Si_2$	4.2, 3.1	Incommensurate		
$TbCu_2Si_2$	13	$(\frac{1}{2},0,\frac{1}{2})$	$\perp\vec{c}$, [110]	8.6
$HoCu_2Si_2$	8	$(\frac{1}{2},0,\frac{1}{2})$	$\perp\vec{c}$, [010]	6.5
$TbFe_2Ge_2$	7.5	Incommensurate		
$DyCo_2Ge_2$	16	(0,0,1)	$\parallel\vec{c}$	9.5
$ErCo_2Ge_2$[c]	4.2	(0,0,1)	$\perp\vec{c}$	
$TbNi_2Ge_2$	16, 9	Incommensurate		
$HoNi_2Ge_2$	6	(0,0,0.76)	$\perp\vec{c}$ (spiral)	~8 (2.1 K)
$TbCu_2Ge_2$	13	$(\frac{1}{2},0,\frac{1}{2})$	$\perp\vec{c}$, [110]	8.6
$HoCu_2Ge$	6.5	$(\frac{1}{2},0,\frac{1}{2})$	$\perp\vec{c}$	

[a]Same $\vec{k}$ and moment direction as in Refs. 40, 45, and 46; $T_N=30$ K in Ref. 45 and 45 K in Refs. 40 and 46; μ (4.2 K)$=8.8\mu_B$ and $8.9\mu_B$ in Refs. 45 and 46, respectively.

[b]Same $\vec{k}$ and moment direction as in Refs. 45, 46, and 48; $T_N=10$, 12, and 13 K in Refs. 46, 48, and 45, respectively.

[c]Same T_N, $\vec{k}$, and moment direction as in Ref. 47.

pounds. The direction of the magnetic moment was determined in full for six compounds and in part for the remaining three compounds. The magnetic configurations of the commensurate structures obtained in the present study are illustrated in Fig. 4. The results of the neutron-diffraction study are given in the following, where the 13 compounds investigated are classified according to the $3d$ transition metal M.

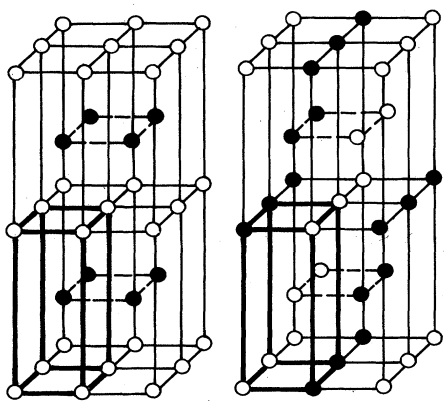

(a) (b)

FIG. 4. Magnetic configurations of the R-sublattice commensurate with the crystallographic lattice of the RM_2X_2 compounds investigated in the present study. Eight crystallographic unit cells are shown (one of them in bold lines). Solid and open circles represent two ferromagnetic sublattices coupled antiferromagnetically. (a) Configuration with $\vec{k}=(0,0,1)$—ferromagnetic (00l) planes coupled antiferromagnetically, and the crystallographic tetragonal unit cell is conserved [corresponding pattern in Fig. 2(a)]. (b) Configuration with $\vec{k}=(\frac{1}{2},0,\frac{1}{2})$—ferromagnetic (101) planes coupled antiferromagnetically, and the unit cell is doubled both in the $\vec{a}$ and $\vec{c}$ directions [corresponding pattern in Fig. 2(b)].

A. Cobalt compounds

$TbCo_2Si_2$, $HoCo_2Si_2$, $DyCo_2Ge_2$, and $ErCo_2Ge_2$ were investigated. All these compounds have a low-temperature pattern similar to the one shown in Fig. 2(a), where all magnetic $\{hkl\}$ reflections with $h+k+l$ even are absent. This pattern is consistent with a type-I antiferromagnetic structure with a propagation vector $\vec{k}=(0,0,1)$ [see Fig. 4(a)]. The absence of the $\{00l\}$ magnetic reflections (except in the erbium compound) is consistent with a magnetic axis along the crystallographic c axis. In $ErCo_2Ge_2$ (at 2.1 K) a magnetic $\{001\}$ reflection is present, indicating canting of the magnetic moment from the c axis, in agreement with the reported[47] angle of 90°.

The transition temperatures (Table II) were measured from the peak intensity versus temperature curves [see Fig. 3(a)] on the magnetic reflections $\{010\}$, $\{012\}$, and $\{111\}$ for $TbCo_2Si_2$, $\{010\}$ for $HoCo_2Si_2$, $\{010\}$ and $\{012\}$ for $DyCo_2Ge_2$, and $\{001\}$ for $ErCo_2Ge_2$.

B. Copper compounds

$TbCu_2Si_2$, $HoCu_2Si_2$, $TbCu_2Ge_2$, and $HoCu_2Ge_2$ were investigated. All these compounds have at 4.2 K, a pattern similar to the one shown in Fig. 2(b), where magnetic $\{h/2\ k\ l/2\}$ reflections appear with odd h and l. This pattern is consistent with a magnetic configuration with propagation vector $\vec{k}=(\frac{1}{2},0,\frac{1}{2})$ [see Fig. 4(b)]. The same configuration was reported for $DyCu_2Si_2$ (Ref. 43) and $DyCu_2Ge_2$ (Ref. 57). From a least-squares best fit of the

calculated to the observed integrated magnetic intensities, the magnetic moment is found to be in the basal plane, perpendicular to the tetragonal c axis. The direction of the moment, except for $HoCu_2Ge_2$, is given in Table II. The compound $TbCu_2Ge_2$ exhibited additional magnetic reflections, incommensurate with the crystallographic lattice, in the low-temperature pattern before annealing, as mentioned in Sec. II A; these additional reflections were absent after the annealing. The low-temperature pattern for $HoCu_2Ge_2$ includes weak additional incommensurate reflections, which are also expected to disappear after annealing. The transition temperatures (Table II) were measured from the peak intensity versus temperature curves [see Fig. 3(b)] on the magnetic reflections $\{\frac{1}{2}\,0\,\frac{1}{2}\}$, $\{\frac{1}{2}\,0\,\frac{3}{2}\}$, and $\{\frac{1}{2}\,1\,\frac{1}{2}\}$ for $TbCu_2Si_2$, $\{\frac{1}{2}\,0\,\frac{1}{2}\}$, $\{\frac{1}{2}\,0\,\frac{3}{2}\}$, and $\{\frac{1}{2}\,0\,\frac{5}{2}\}$ for $HoCu_2Si_2$, and $\{\frac{1}{2}\,0\,\frac{1}{2}\}$ for $TbCu_2Ge_2$ and $HoCu_2Ge_2$.

C. Nickel compounds

$HoNi_2Si_2$, $TbNi_2Ge_2$, and $HoNi_2Ge_2$ were investigated. The room-temperature neutron-diffraction patterns are in agreement with the crystallographic structures. However, the low-temperature patterns (at 4.2 and 2.1 K) show the existence of incommensurate structures. These have not yet been solved for $HoNi_2Si_2$ and $TbNi_2Ge_2$. In these compounds the magnetic reflections yield two transition temperatures in each: 4.2 and 3.1 K in $HoNi_2Si_2$ and 16 and 9 K in $TbNi_2Ge_2$. In $HoNi_2Ge_2$ the room-temperature and low-temperature patterns indicate no detectable change in the lattice parameters ($a=4.021$ Å and $c=9.757$ Å). The incommensurate magnetic structure at 2.1 K is consistent with a spiral having a propagation vector $\vec{k}=(0,0,0.76)$ and a turning axis along this propagation vector. The magnetic moment is $\sim 8\mu_B$ and is perpendicular to the c axis. The 2.1 K pattern is shown in Fig. 2(c). The transition temperature (Table II) was deduced from peak intensity versus temperature curves for the $\{000\}^{\pm}$ and $\{002\}^{-}$ magnetic reflections [$T_N=(6\pm1)$ K; see Fig. 3(c)].

D. Iron compounds

$TbFe_2Si_2$ and $TbFe_2Ge_2$ were investigated. The room-temperature neutron-diffraction patterns are in agreement with the published crystallographic structures. However, the low-temperature patterns (at 4.2 and 2.1 K) show the existence of the incommensurate structures, to be solved in the future. The transition temperatures (Table II) were derived from the most intense magnetic reflections, at $2\theta=16.1°$ for $TbFe_2Si_2$ and $2\theta=7.6°$ for $TbFe_2Ge_2$.

IV. DISCUSSION

The magnetic system in the RM_2X_2 compounds consists of localized $4f$ moments on the R ions and localized $3d$ moments of the M ions. The localized moments interact directly, and indirectly via the itinerant s electrons. The direction and magnitude of the ordered magnetic moments are affected by the local crystalline electric field (CEF). By discussing the experimental results we shall be able to assess which of the above interactions plays a dominant role in determining the magnetic properties of these compounds.

The RM_2X_2 compounds are paramagnetic at room temperature and undergo a transition to antiferromagnetic ordering of the R sublattice at low temperatures (Table III). Magnetic ordering of the M sublattice was not found in any of the compounds investigated in the present study. One should, however, recognize the fact that the analyses of the diffraction patterns are not sensitive to small magnetic moments on the M sublattice. Isostructural compounds, with R replaced by La, Lu, and Y (diamagnetic ions), show Pauli paramagnetism down to 4.2 K, with no sign of magnetic ordering.[18] The Néel temperatures and magnetic structure parameters of the RM_2X_2 compounds, obtained in the present work and in other works,[13,18,20,21,24–26,28,29,41,43–49,53,57,60,62–65] are summarized in Table III.

The reported transition temperatures of the RM_2X_2 compounds (Table III) are shown schematically as a function of R and M, separately for Si and Ge, in Fig. 5. The highest transition temperatures are found in the cobalt compounds. Upon variation of R, the transition temperature follows the de Gennes function,[69] $\Gamma J(J+1)(g-1)^2$, for $M=$ Fe, Co, and Ni, whereas it seems to deviate from this function in the copper compounds. The de Gennes function behavior indicates that the dominant magnetic interaction is indirect, via polarization of the conduction electrons, namely the Ruderman-Kittel-Kasuya-Yosida (RKKY) interaction.[69]

The various low-temperature magnetic structures found in the RM_2X_2 compounds belong to several magnetic configurations. The magnetic configuration varies with the $3d$ element M, and seems to be almost independent of the R ion (Table III). The iron and nickel compounds have mostly incommensurate $\vec{k}$ vectors for the magnetic structures, except for $ErFe_2Si_2$, with $\vec{k}=(0,0,\frac{1}{2})$,[53] and $TbNi_2Si_2$, with $\vec{k}=(\frac{1}{2},\frac{1}{2},0)$.[45] The cobalt compounds have $\vec{k}=(0,0,1)$, hence changing the body-centered translation into an antitranslation [Fig. 4(a)]. On the other hand, the copper compounds have $\vec{k}=(\frac{1}{2},0,\frac{1}{2})$, hence

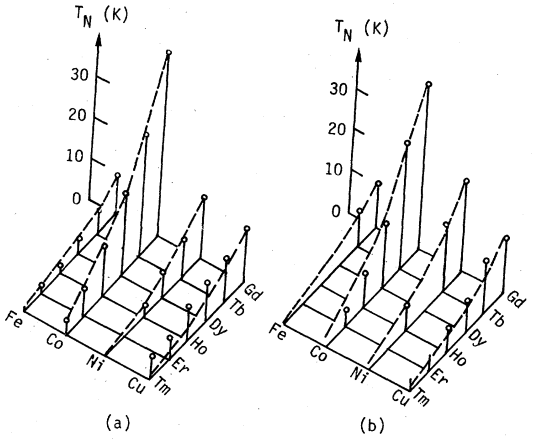

FIG. 5. Transition temperature T_N (circles) of the RM_2X_2 compounds plotted as a function of R for the various M, with the corresponding de Gennes functions (dashed lines). (a) $X=$Si; (b) $X=$Ge.

TABLE III. Magnetic structure data for the 48 RM_2X_2 compounds. First row: transition temperature T_N (in K); second row: propagation vector $\vec{k}$; third row: magnetic moment direction ($\not\propto$ denotes angle with a crystallographic axis); fourth row: magnetic moment magnitude at 4.2 K (in μ_B) (or at lower temperature, when indicated). Data where no references are indicated were obtained in the present study. Incommen. denotes incommensurate magnetic structure.

	RM_2Si_2				RM_2Ge_2			
R	RFe_2Si_2	RCo_2Si_2	RNi_2Si_2	RCu_2Si_2	RFe_2Ge_2	RCo_2Ge_2	RNi_2Ge_2	RCu_2Ge_2
Gd	q[a]	44[b], 46.4[a]	11.6,[a] 15.5[c]	12÷14[d]	11[e,f,g]	40[h]	22[e]	12,[i] 14[e]
	90° $\not\propto \vec{c}$ [a]	78° $\not\propto \vec{c}$ [a]	70° $\not\propto \vec{c}$ [a]	90° $\not\propto \vec{c}$ [a]				
Tb	10.5	46	10[j]	13	7.5	31[k]	16; 9	13
	Incommen.	(0,0,1)	$(\frac{1}{2},\frac{1}{2},0)$[j]	$(\frac{1}{2},0,\frac{1}{2})$	Incommen.	(0,0,1)[k]	Incommen.	$(\frac{1}{2},0,\frac{1}{2})$
		$\|\|\vec{c}$	$\|\|\vec{c}$ [j]	$\perp\vec{c}$, [110]		$\|\|\vec{c}$ [k]		$\perp\vec{c}$, [110]
		9.2	8.8[j]	8.6		8.84[k]		8.6
Dy	3.8[l]	21[m]	7,[c] <4.2[n]	11[m]		16		8[i,o]
		(0,0,1)[m]		$(\frac{1}{2},0,\frac{1}{2})$[m]		(0,0,1)		$(\frac{1}{2},0,\frac{1}{2})$[o]
		$\|\|\vec{c}$ [m]		$\perp\vec{c}$, [010][m]		$\|\|\vec{c}$		70° $\not\propto c$, 30° $\not\propto \vec{a}$ [o]
		9.5[m]		8.3[m]		9.5		8 (3 K)[o]
Ho	2.2[l]	10.2	4.2; 3.1	8		8.5[k]	6	6.5
		(0,0,1)	Incommen.	$(\frac{1}{2},0,\frac{1}{2})$		(0,0,1)[k]	(0,0,0.76)	$(\frac{1}{2},0,\frac{1}{2})$
		$\|\|\vec{c}$		$\perp\vec{c}$, [010]		$\|\|\vec{c}$ [k]	$\perp\vec{c}$, spiral	$\perp\vec{c}$
		8.1,[j] 9.8,[p] 10.4[q]		6.5		8.12÷8.28[k]	~8 (2.1 K)	
Er	2.6[r,s]	6,[b,t] 11[q]		2.0÷4.8[d]	<4.2[u]	~4.2		<4.2[i]
	$(0,0,\frac{1}{2})$[r]	(0,0,1)[q,u]				(0,0,1)		
	$\|\|\vec{c}$ [r]	56.2° $\not\propto \vec{c}$, [t] $\perp\vec{c}$ [q]				$\perp\vec{c}$		
	7.4 (1.8 K)[r]	6.75,[t] 8.7[q]				7.3 (2.0 K)[v]		
Tm	<1.3[l]	3[w]		2.8,[x] 7.0[d]		<4.2[h]		<4.2[i]
		(0,0,1)[w]						
		$\perp\vec{c}$ [w]						
		6.2 (2.0 K)[w]						

[a]Reference 60.
[b]Reference 25.
[c]Reference 26.
[d]Reference 29.
[e]Reference 13.
[f]Reference 20.
[g]Reference 21.
[h]Reference 18.
[i]Reference 28.
[j]Reference 45.
[k]Reference 41.
[l]Reference 65.
[m]Reference 43.
[n]Reference 62.
[o]Reference 57.
[p]Reference 48.
[q]Reference 46.
[r]Reference 53.
[s]Reference 64.
[t]Reference 44.
[u]Reference 24.
[v]Reference 47.
[w]Reference 49.
[x]Reference 63.

doubling the tetragonal unit cell in the $\hat{x}$ (or $\hat{y}$) and $\hat{z}$ directions [Fig. 4(b)]. This interesting dependence of the magnetic configuration of the R sublattice on the M ion is perhaps through the density of the conduction electrons, contributed by the M ions.

The direction of the magnetic moment is not fixed for a given M. We believe that the direction is determined by the interaction between the crystalline electric field and the magnetic R ions. We have evidence of the existence of such an interaction in CEF transitions, which have been observed with inelastic neutron scattering.[70] The magnitude of the magnetic moments is somewhat smaller than the corresponding free-R-ion values. Most likely, this is also due to CEF effects.

The actinide compounds AB_2X_2 (A denoting an actinide) exhibit, in general, magnetic structures similar to those in the LnB_2X_2 compounds (see Refs. 36, 39, 42, and 51). The systematics of the magnetic structures in the actinide compounds has not yet been discussed. We may, however, point out in passing that the transition temperatures for the actinide compounds are generally higher than those in the corresponding lanthanide compounds.

ACKNOWLEDGMENTS

The authors are indebted to Dr. J. Gal for his interest in the present study and his help in sample preparations, and to Mr. S. Fredo and Mr. H. Ettedgui for preparation of the samples and technical assistance. This work was supported in part by the Fund for Basic Research, administered by the Israel Academy of Sciences and Humanities.

[1]Z. Ban and M. Sikirica, Acta Crystallogr. **18**, 594 (1965).
[2]Z. Ban and M. Sikirica, Z. Anorg. Allg. Chem. **356**, 96 (1967).
[3]W. Rieger and E. Parthe, Monatsh. Chem. **100**, 444 (1969).
[4]I. Mayer and I. Felner, J. Less-Common Met. **29**, 25 (1972).
[5]I. Mayer and J. Cohen, J. Less-Common Met. **29**, 221 (1972).
[6]I. Mayer, J. Cohen, and I. Felner, J. Less-Common Met. **30**, 181 (1973).
[7]W. M. McCall, K. S. V. L. Narasimhan, and R. A. Butera, J. Appl. Crystallogr. **6**, 301 (1973).
[8]R. Ballestracci, C. R. Acad. Sci. Ser. B **282**, 291 (1976); R. Ballestracci and G. Astier, *ibid.* **286**, 109 (1978).
[9]I. Mayer and I. Felner, J. Phys. Chem. Solids **38**, 1031 (1977).
[10]I. Mayer and P. D. Yetor, J. Less-Common Met. **55**, 171 (1977).
[11]R. Marazza, R. Ferro, G. Rambaldi, and G. Zanicchi, J. Less-Common Met. **53**, 193 (1977).
[12]D. Rossi, R. Marazza, and R. Ferro, J. Less-Common Met. **58**, 203 (1978).
[13]I. Felner and I. Nowik, J. Phys. Chem. Solids **39**, 767 (1978).
[14]D. Rossi, R. Marazza, D. Mazzone, and R. Ferro, J. Less-Common Met. **59**, 79 (1978).
[15]K. Hiebl, C. Horvath, P. Rogl, and M. J. Sienko, Solid State Commun. **48**, 211 (1983); J. Magn. Magn. Mater. **37**, 287 (1983).
[16]*Symmetry Groups,* Vol. I of *International Tables for X-Ray Crystallography,* edited by N.F.M. Henry and K. Lonsdale (Kynoch, Birmingham, England, 1969), pp. 241–242.
[17]L. Omejec and Z. Ban, Z. Anorg. Allg. Chem. **380**, 111 (1971).
[18]W. M. McCall, K. S. V. L. Narasimhan, and R. A. Butera, J. Appl. Phys. **44**, 4724 (1973).
[19]I. Felner, J. Phys. Chem. Solids **36**, 1063 (1975).
[20]I. Felner, I. Mayer, A. Grill, and M. Schieber, Solid State Commun. **16**, 1005 (1975).
[21]S. K. Malik, S. G. Sankar, V. U. S. Rao, and R. Obermyer, in *Magnetism and Magnetic Materials—1975 (Philadelphia),* proceedings of the 21st Annual Conference on Magnetism and Magnetic Materials, edited by J. J. Becker, G. H. Lander, and J. J. Rhyne (AIP, New York, 1976), p. 585.
[22]K. S. V. L. Narasimhan, V. U. S. Rao, W. E. Wallace, and I. Pop, in *Magnetism and Magnetic Materials—1975 (Philadelphia),* Ref. 21, p. 594.
[23]J. Gal, M. Kroupp, Z. Hadari, and I. Nowik, Solid State Commun. **20**, 421 (1976); **20**, 515 (1976).
[24]S. G. Sankar, S. K. Malik, V.U.S. Rao, and R. Obermyer, in *Magnetism and Magnetic Materials—1976 (Joint MMM-Intermag Conference, Pittsburgh),* partial proceedings of the First Joint MMM-Intermag Conference, edited by J. J. Becker and G. H. Lander (AIP, New York, 1977), p. 236.
[25]J. K. Yakinthos, Ch. Rousti, and P. F. Ikonomou, J. Less-Common Met. **72**, 205 (1980).
[26]J. K. Yakinthos and P. F. Ikonomou, Solid State Commun. **34**, 777 (1980).
[27]Ch. Rousti and J. K. Yakinthos, Phys. Status Solidi A **68**, K153 (1981).
[28]P. A. Kotsanidis and J. K. Yakinthos, Solid State Commun. **40**, 1041 (1981).
[29]W. Schlabitz, J. Baumann, G. Neumann, D. Plümacher, and K. Reggentin, in *Crystalline Electric Field Effects in f-Electron Magnetism,* edited by R. P. Guertin, W. Suski, and Z. Zolnierek (Plenum, New York, 1982), p. 289.
[30]M. Kolenda, A. Szytula, and A. Zygmunt, in *Crystalline Electric Field Effects in f-Electron Magnetism,* Ref. 29, p. 309.
[31]J. Baumann, W. Hoheisel, W. Krause, D. Müller, G. Neumann, H. Zahel, and W. Schlabitz, in "13èmes Journées des Actinides, Elat, Israel, 1983," published as NRC-Negev Internal Report No. NRCN(GP)-030.
[32]I. Felner and I. Nowik, Solid State Commun. **47**, 831 (1983).
[33]H. Pinto and H. Shaked, Phys. Rev. B **7**, 3261 (1973).
[34]Z. Ban, L. Omejec, A. Szytula, and Z. Tomkowicz, Phys. Status Solidi A **27**, 333 (1975).
[35]H. Pinto, M. Melamud, and E. Gurewitz, Acta Crystallogr. Sect. A **35**, 533 (1979).
[36]C. H. de Novion, J. Gal, and J. L. Buevoz, J. Magn. Magn. Mater. **21**, 85 (1980).
[37]A. Szytula, J. Leciejewicz, and H. Bińczycka, Phys. Status Solidi A **58**, 67 (1980).
[38]J. Leciejewicz, H. Ptasiewicz-Bak, and A. Zygmunt, Phys. Status Solidi A **51**, K71 (1979); H. Ptasiewicz-Bak, J. Leciejewicz, and A. Zygmunt, J. Phys. F **11**, 1225 (1981).
[39]J. Leciejewicz, in *Crystalline Electric Field Effects in f-Electron Magnetism,* Ref. 29, p. 279.
[40]J. Leciejewicz, S. Siek, A. Szytula, and A. Zygmunt, in *Crystalline Electric Field Effects in f-Electron Magnetism,* Ref. 29, p. 327.
[41]H. Pinto, M. Melamud, and H. Shaked, in *Neutron Scattering—1981 (Argonne National Laboratory),* edited by J. Faber, Jr. (AIP, New York, 1982), p. 315.
[42]J. Leciejewicz, L. Chelmicki, and A. Zygmunt, Solid State Commun. **41**, 167 (1982).
[43]H. Pinto, M. Melamud, J. Gal, H. Shaked, and G. M. Kalvius, Phys. Rev. B **27**, 1861 (1983).
[44]J. K. Yakinthos, Ch. Rousti, and P. Schobinger-Papamantellos, J. Magn. Magn. Mater. **30**, 355 (1983).
[45]V. N. Nguyen, F. Tcheou, J. Rossat-Mignod, and R. Ballestracci, Solid State Commun. **45**, 209 (1983).
[46]J. Leciejewicz, M. Kolenda, and A. Szytula, Solid State Commun. **45**, 145 (1983).
[47]J. Leciejewicz, A. Szytula, and A. Zygmunt, Solid State Commun. **45**, 149 (1983).
[48]P. Schobinger-Papamantellos, Ch. Rousti, and J. K. Yakinthos, J. Phys. Chem. Solids **44**, 875 (1983).
[49]J. Leciejewicz and A. Szytula, Solid State Commun. **48**, 55 (1983).
[50]M. Slaski, J. Leciejewicz, and A. Szytula, J. Magn. Magn. Mater. **39**, 268 (1983).
[51]L. Chelmicki, J. Leciejewicz, and A. Zygmunt, Solid State Commun. **48**, 177 (1983).
[52]A. Szytula, W. Bażela, and J. Leciejewicz, Solid State Commun. **48**, 1053 (1983).
[53]J. Leciejewicz, S. Siek, and A. Szytula, J. Magn. Magn. Mater. **40**, 265 (1984).
[54]B. H. Grier, J. M. Lawrence, V. Murgai, and R. D. Parks, Phys. Rev. B **29**, 2664 (1984).
[55]S. Quezel, J. Rossat-Mignod, B. Chevalier, P. Lejay, and J. Etourneau, Solid State Commun. **49**, 685 (1984).
[56]M. Melamud, H. Pinto, I. Felner, and H. Shaked, J. Appl. Phys. **55**, 2034 (1984).
[57]P. A. Kotsanidis, J. K. Yakinthos, and E. Roudaut, Solid State Commun. **50**, 413 (1984).
[58]E. R. Bauminger, D. Froindlich, I. Nowik, S. Ofer, I. Felner, and I. Mayer, Phys. Rev. Lett. **30**, 1053 (1973).
[59]E. A. Görlich, A. Z. Hrynkiewicz, K. Latka, R. Kmiec, A. Szytula, and K. Tomala, J. Phys. (Paris) **40**, C2-656 (1979).
[60]I. Nowik, I. Felner, and M. Seh, J. Magn. Magn. Mater. **15-18**, 1215 (1980).
[61]W. Potzel, J. Moser, G. M. Kalvius, C. H. de Novion, J. C. Spirlet, and J. Gal, Phys. Rev. B **24**, 6762 (1981).
[62]E. A. Görlich, R. Kmiec, B. Janus, and A. Szytula, in *Crystal-*

line Electric Field Effects in f-Electron Magnetism, Ref. 29, p. 301.

[63]G. A. Stewart and J. Zukrowski, in *Crystalline Electric Field Effects in f-Electron Magnetism,* Ref. 29, p. 319.

[64]A. M. Umarji, D. R. Noakes, P. J. Viccaro, G. K. Shenoy, A. T. Aldred, and D. Niarchos, J. Magn. Magn. Mater. **36**, 61 (1983).

[65]D. R. Noakes, A. M. Umarji, and G. K. Shenoy, J. Magn. Magn. Mater. **39**, 309 (1983).

[66]A. M. Umarji, G. K. Shenoy, D. R. Noakes, and S. Dattagupta, J. Appl. Phys. **55**, 2297 (1984).

[67]B. Batlogg, J. P. Remeika, A. S. Cooper, and Z. Fisk, J. Appl. Phys. **55**, 2001 (1984).

[68]A. J. Freeman and R. E. Watson, Acta Crystallogr. **14**, 231 (1961).

[69]C. Kittel, *Quantum Theory of Solids* (Wiley, New York, 1963).

[70]M. Melamud and H. Shaked (unpublished).